

General Disclaimer

One or more of the Following Statements may affect this Document

- This document has been reproduced from the best copy furnished by the organizational source. It is being released in the interest of making available as much information as possible.
- This document may contain data, which exceeds the sheet parameters. It was furnished in this condition by the organizational source and is the best copy available.
- This document may contain tone-on-tone or color graphs, charts and/or pictures, which have been reproduced in black and white.
- This document is paginated as submitted by the original source.
- Portions of this document are not fully legible due to the historical nature of some of the material. However, it is the best reproduction available from the original submission.

LEGAL NOTICE

This report was prepared as an account of Government sponsored work. Neither the United States, nor the Commission, nor any person acting on behalf of the Commission:
A. Makes any warranty or representation, expressed or implied, with respect to the accuracy, completeness, or usefulness of the information contained in this report, or that the use of any information, apparatus, method, or process disclosed in this report may not infringe privately owned rights; or
B. Assumes any liabilities with respect to the use of, or for damages resulting from the use of any information, apparatus, method, or process disclosed in this report.
As used in the above, "person acting on behalf of the Commission" includes any employee or contractor of the Commission, or employee of such contractor, to the extent that such employee or contractor of the Commission, or employee of such contractor prepares, disseminates, or provides access to, any information pursuant to his employment or contract with the Commission, or his employment with such contractor.

 **Astronuclear
Laboratory**
WANL-TME-1492
AUGUST, 1966

SUBMITTED BY:

Westinghouse Electric Corporation
Astronuclear Laboratory
Pittsburgh, Pennsylvania 15236

CFSH PRICES

H.C. \$ 2.00; MN. .50

RELEASED FOR ANNOUNCEMENT
IN NUCLEAR SCIENCE ABSTRACTS

PROGRESS REPORT ON NEUTRON INTERFERENCE SCATTERING
IN CRYSTALLINE SOLIDS

UNCLASSIFIED NERVA RESEARCH
AND DEVELOPMENT REPORT.

PREPARED BY:

A. S. Johnston
A. S. Johnston
Physics & Mathematics

INFORMATION CATEGORY

APPROVED BY:

unclassified
DW Drawbaugh 8/19/66
Authorized Classifier - Date

DW Drawbaugh
D. W. Drawbaugh, Manager
Reactor Physics & Mathematics

CONTENTS

	<u>Page</u>
I. INTRODUCTION	1
II. ELASTIC SCATTERING	2
III. INELASTIC SCATTERING	9
1. One Phonon Exchanges	9
2. Multiphonon Processes	13
3. Scattering Law	14
4. Consideration for Coherent Calculation	16
IV. LATTICE DYNAMICS AND SCATTERING LAW	22
1. General	22
2. Beryllium	23
3. Graphite	27
4. Method of Calculating the Frequency Distribution $g(\omega)$	28
V. CONCLUSIONS	30
REFERENCES	31

ABSTRACT

The literature has been studied to determine two things; first to determine the principles, the methods, and the current results of calculations of inelastic neutron scattering from polycrystalline beryllium and graphite, and secondly to determine the agreement that has been obtained between calculations and measurements of the elastic and inelastic neutron scattering cross section. The principles by which the inelastic scattering cross section is calculated are outlined, some of the Born-Von Karman models proposed for hexagonal lattices are described, and methods of numerically evaluating the inelastic scattering cross section formulas are discussed.

I. INTRODUCTION

Interference scattering of neutrons from polycrystalline graphite and beryllium may be an important factor in the operation of a NERVA type reactor. This is especially true since the beryllium operates quite cold. The work which this progress report concerns is directed toward understanding the effect of interference scattering of neutrons by beryllium and graphite.

The work, to date, has consisted of a study of existing calculations and experimental data. In this progress report methods used to calculate the cross section for elastic and inelastic scattering of neutrons from crystalline solids are discussed. The derivation of relevant formulas are sketched, and points where the more important approximations enter are noted.

Calculation of one phonon process for polycrystalline solids is explained. Present calculations of this cross section and available experimental data are discussed.

II. ELASTIC SCATTERING

The differential cross section for scattering neutrons from crystalline solids is given in the Born approximation as;

$$G = \left(\frac{m_0}{\hbar^2 2\pi} \right)^2 \frac{k_2}{k_1 N} \langle f | M | i \rangle^2. \quad (1)$$

For elastic neutron scattering from a crystal lattice using the Fermi pseudopotential and after integration over space coordinates, including an ensemble average over initial states this becomes¹:

$$G_0 = \left(\frac{m_0}{\hbar 2\pi} \right)^2 \frac{k_2}{k_1 N} \left(\frac{2\pi\hbar^2}{m_0} \right)^2 \sum_{\eta_1=0}^{\infty} \sum_{\eta_2=0}^{\infty} \cdots \sum_{\eta_N=0}^{\infty} \left(\prod_{j=1}^N P(\eta_j) \right) \\ \times \left| \sum_{\sigma} a_{\sigma} e^{i(\bar{k}_1 - \bar{k}_2) \cdot \sigma} \prod_{j=1}^N F_{\eta_j n_j} \right|^2 \quad (2)$$

$$F_{\eta_j n_j} = \langle \eta_j | e^{i Q_j \sigma a_j + Q_j^* \sigma a_j^*} | \eta_j \rangle \quad (3)$$

$$P(\eta_j) = \frac{e^{-(\eta_j + \frac{1}{2}) \frac{\hbar \omega_j}{k_0 T}}}{\sum_{\eta_j=0}^{\infty} e^{-(\eta_j + \frac{1}{2}) \frac{\hbar \omega_j}{k_0 T}}} = \left(1 - e^{-\frac{\hbar \omega_j}{k_0 T}} \right) e^{-\eta_j \frac{\hbar \omega_j}{k_0 T}} \quad (4)$$

In expression (1) and (2) the symbols are defined as follows:

G_0 = elastic, single crystal, differential neutron scattering cross section

m_0 = mass of the neutron

N = number of unit cells in the crystal

k_1 = magnitude of the wave vector of the incident neutron

\vec{k}_1 = wave vector of the incident neutron

k_2 = magnitude of the wave vector of the scattered neutron

\vec{k}_2 = wave vector of the scattered neutron

$\langle f|M|i\rangle^2$ = indicates the square of the appropriate matrix element

$|f\rangle$ is the final state

$|i\rangle$ is the initial state

$\sum_{n_j=0}^{\infty}$ = is the sum over all occupation numbers n_j of the j^{th} normal mode and branch of the crystal dispersion relation.

$P(n_j)$ probability of occupation of the n_j^{th} level of the j^{th} normal mode

$\prod_{j=1}^N P(n_j)$ constitutes the weighting for a particular choice of each n_j for an ensemble average

σ is used to indicate unit cells of the crystal

$\vec{\sigma}$ = equilibrium position of the unit cells of the crystal lattice. For a Bravais lattice $\vec{\sigma}$ gives the equilibrium position of the σ^{th} atom. For a crystal with a basis the position of an atom is given by:

$$R_{\sigma,b} = \vec{\sigma} + \vec{b} + \vec{u}$$

\vec{b} = the basis vector ($\vec{b} = 0$ for a Bravais lattice)

\vec{u} = time dependent displacement from the equilibrium position in the lattice

a_σ is the bound atom scattering length of the atom σ .

$a_\sigma = \left(\frac{A+1}{A}\right) a_{\text{free}}$. Here a_{free} is the free atom scattering length.

$|n_j\rangle$ = is a single particle Harmonic oscillator state of energy $\hbar\omega_j n_j$.

a_j and a_j^* are annihilation and creation operators for the state $|n_j\rangle$

$$a_j |n_j\rangle = \sqrt{n_j} |n_j - 1\rangle$$

$$a_j^* |n_j\rangle = \sqrt{n_j + 1} |n_j + 1\rangle$$

$$a_j a_j^* - a_j^* a_j = 1$$

$$Q_{j\sigma} = \sqrt{\frac{\hbar^2}{2M_N \hbar\omega_j}} \sum_s \left[(\bar{k}_1 - \bar{k}_2) \cdot \bar{E}_s^f \right] e^{i \vec{r}_j \cdot \vec{\sigma}}$$

s = represents the polarization of a lattice wave

\bar{E}_s^f = the polarization vector for mode f

$\hbar\omega_j$ = energy of a lattice vibration of mode and branch j .

\vec{r}_j = wave vector of a lattice wave of mode and branch j .

k_1 = Boltzmann constant

T = temperature of the crystal.

In equation (2) \vec{u}_σ has been expanded in terms of normal modes of the crystal and written in terms of annihilation and creation operators.

The expression 2 has been evaluated (references 1,2,3) to give the differential cross section.

$$G_0 = \frac{R e^{-2W}}{4\pi} + \frac{2\pi^2 S e^{-2W}}{B} \delta(\vec{K} - 2\pi \vec{\tau}) \quad (5)$$

$$2W = \sum_{j,S} \left(\frac{\hbar^2}{2MN} \right) \left[(\vec{k}_1 - \vec{k}_2) \cdot \vec{E}_S \right] \frac{\coth \frac{\hbar \omega_j}{2k_B T}}{\hbar \omega_j} \quad (6)$$

$$R = 4\pi (\overline{a^2} - \bar{a}^2) \quad \text{the incoherent average of scattering amplitudes}^1 \quad (7)$$

$$S = 4\pi \bar{a}^2 \quad \text{the coherent average of scattering amplitudes}^1 \quad (8)$$

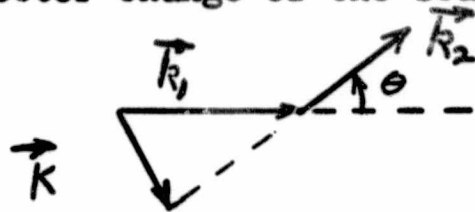
The new symbols in expressions (5), (6), (7), and (8) are:

R = incoherent average of scattering amplitudes. The term in expression 5 containing R gives the elastic incoherent scattering cross section.

S = coherent average of scattering amplitudes. The term in expression 5 containing S gives the elastic scattering cross section (diffraction scattering).

B = volume of the unit cell of the direct lattice

$\vec{K} = \vec{k}_1 - \vec{k}_2$ is the wave vector change of the scattered neutron



θ = scattering angle, between \vec{k}_1 and \vec{k}_2

$\vec{\tau}$ = reciprocal lattice vector associated with the lattice planes which bisect θ .

Since the purpose of this report is to discuss only beryllium and graphite scattering cross sections, the incoherent cross section can be dropped from consideration. This is because⁴ R is measured to be negligibly small for both graphite and beryllium.

Equation 5 gives the elastic differential coherent scattering cross section as:

$$\frac{d^2 \sigma_{o,coh}^{\tau}}{d\Omega} = \int \frac{2\pi^2 e^{-2W}}{B} \delta(\vec{K} - 2\pi \vec{\tau}) \quad (9)$$

$d\Omega$ is the solid angle into which the neutron is scattered.

Equation 9 holds for a single crystal small enough so that extinction effects are not appreciable (i.e. a microcrystal). The superscript τ means that the scattering occurs from the crystal planes denoted by $\vec{\tau}$.

The cross section for a polycrystalline solid can be obtained by averaging equation 9 over all orientation of $\vec{\tau}$, (references 1,5), giving for the polycrystalline cross section for the crystal planes denoted by τ ;

$$\frac{d^2 \sigma_{o,coh}^{\tau}}{d\Omega} = \frac{\int e^{-2W}}{8\pi B \tau^2} \delta(2k, \sin \frac{\theta}{2} - 2\pi \tau) \quad (10)$$

The total coherent elastic scattering cross section for lattice planes τ is obtained from equation 10 by integrating over $d\Omega^5$.

$$\sigma_{o,coh}^{\tau} = \frac{\int \pi}{2 B \tau k^2} e^{-2W} \quad (11)$$

The total coherent elastic scattering cross section is then obtained by summing over lattice planes, or more conveniently, over reciprocal lattice vectors.

$$\sigma_{o,coh} = \frac{5\pi}{2B k_1^2} \sum_{2\pi\tau \leq \frac{2}{\lambda}} \frac{1}{\tau} e^{-2W} \quad (12)$$

$$\lambda = \frac{2\pi}{k_1} = \text{wavelength of the neutron.}$$

In going from equation 5 to equation 12 it has been assumed that W is independent of the angle between \vec{K} , and $\vec{\tau}$. However W depends on $\sum_S (\vec{K} \cdot \vec{E}_S)^2$, and in usual approximations this becomes proportional to $(\vec{K})^2$. In equation 12 $(\vec{K})^2$ in W must be replaced by $(2\pi\tau)^2$ as a consequence of the delta function of equation 10. The sum over modes in equation 6 for W is usually evaluated by an integral over the frequency spectrum. See equations 39 through 42.

If an expansion of the total cross section in terms of Legendre polynomials $P_n(\cos \theta)$ is desired, the n^{th} coefficient can be obtained from equation 10 by first multiplying by $P_n(\cos \theta)$ before integrating over the solid angle.

For a non-Bravais lattice, the form factor must be included in equation 12. If the crystal is composed of n molecules each containing m atoms then reference 1 gives the following substitutions to include the form factor. Here hkl are Miller indices of a plane and X_{jr} , Y_{jr} , Z_{jr} are the coordinates of an atom in the lattice.

$$R e^{-2W} \rightarrow 4\pi \sum_{r=1}^m n a_r^2 e^{-2W_r} \quad (13a)$$

$$(S e^{-2W})_{hkl} \rightarrow 4\pi \left| \sum_{j=1}^n \sum_{r=1}^m a_r e^{2\pi i(hX_{jr} + kY_{jr} + lZ_{jr})} e^{-W_r} \right|^2 \quad (13b)$$

W depends on the mass of the atom and so must carry the subscript W_r . Equation 12 becomes for a lattice with a basis:

$$\sigma_{0,coh} = \frac{4\pi^2}{2Bk_l^2} \sum_{\vec{\tau} \leq \frac{2\pi}{\lambda}} \frac{1}{\tau} \left| \sum_{\ell} \sum_{r=1}^m a_r e^{2\pi i(hX_{\ell r} + kY_{\ell r} + lZ_{\ell r})} e^{-W_r} \right|^2 \quad (14)$$

The sum over $\vec{\tau}$ includes all values of $\vec{\tau}$ since no multiplicity factor is included in equation 14 to take account of values of $\vec{\tau}$ which, for different values of hkl , are equal in magnitude.

III. INELASTIC SCATTERING

1. One Phonon Exchanges

In the Born approximation the differential scattering cross section for single phonon absorption by a neutron scattered from an initial state \vec{k}_1 to a final state \vec{k}_2 is, (reference 1);

$$G_{01} = \left(\frac{m_0}{2\pi\hbar^2}\right)^2 \frac{k_2}{Nk_1} \left(\frac{2\pi\hbar^2}{m_0}\right)^2 \sum_{n_1=0}^{\infty} \dots \sum_{n_N=0}^{\infty} \sum_S \left(\prod_{j=1}^N P(n_j) \right) \times \left| \sum_{\sigma} a_{\sigma} e^{i(\vec{k}_1 - \vec{k}_2 + \vec{f}_1) \cdot \vec{\sigma}} \langle n_1 - 1 | e^{i(Q_1 \sigma a_1 + Q_1^* \sigma^* a_1^*)} | n_1 \rangle \right. \quad (15)$$

$$\left. \times \prod_{j=2}^N \langle n_j | e^{i(Q_j \sigma a_j + Q_j^* \sigma^* a_j^*)} | n_j \rangle \right|^2$$

G_{01} is the cross section for one phonon absorption by a neutron. All of the other symbols have the same meaning as in equation 2.

Equation 15 is evaluated in reference 1 and shown to simplify to:

$$G_{01} = \frac{\hbar^2}{8\pi MN\hbar\omega} \frac{k_2 e^{-2\omega}}{k_1} \sum_S \left[(\vec{k}_1 - \vec{k}_2) \cdot \vec{f}_S^f \right]^2 \frac{1}{e^{\frac{\hbar\omega}{kT}} - 1} \times \left[R + \frac{(2\pi)^3}{B} S S (\vec{k}_1 - \vec{k}_2 + \vec{f} - 2\pi \vec{\tau}) \right] \quad (16)$$

$\hbar\omega$ = the energy of the absorbed phonon and is positive.

Conservation of energy requires:

$$E_2 = E_1 + \hbar\omega \quad (17)$$

where:

$$E_1 = \frac{\hbar^2 k_1^2}{2m_0} \quad E_2 = \frac{\hbar^2 k_2^2}{2m_0}$$

E_1 and E_2 are the neutron kinetic energy before and after scattering. Equation 16 is for phonon absorption (neutron up-scatter).

The delta function in equation 16 includes the conservation of crystal momentum for coherent scattering as,

$$\vec{k}_1 - \vec{k}_2 = 2\pi\vec{\tau} - \vec{f} \quad (18)$$

We will consider only the coherent scattering term of equation 16 because measurements show R for graphite⁴ and beryllium⁴ to be negligibly small.

Next the development to the total one phonon absorption cross section is sketched, and the "incoherent approximation" is illustrated.

The coherent term of equation 16 is summed over all orientations of \vec{k}_2 and averaged over all directions of the reciprocal lattice vector in order to obtain the total one phonon polycrystalline cross section for absorption of a phonon of wave vector \vec{f} , contributed by the reciprocal lattice point $\vec{\tau}$, (references 1,5). The result is,

$$\frac{d\sigma_{\text{coh}}(E_1 \rightarrow E_2)^{\tau}}{dE_2} = \frac{\pi^2 \hbar S}{2MN B k_1^2} \frac{1}{\hbar\omega(e^{\hbar\omega/RT} - 1)} |2\pi\vec{\tau} - \vec{f}| e^{-2W} \quad (19)$$

$\frac{d\sigma(E_1 \rightarrow E_2)}{dE_2}$ is the one phonon absorption cross section integrated over outgoing neutron directions, for a phonon of wave vector \vec{f} for a polycrystalline solid for the contribution of one point ($\vec{\tau}$) of the reciprocal lattice. It is differential in final neutron energy. Any dependence of W on the angle of scattering has been neglected.

In order to obtain the total one phonon absorption cross section, equation 19 must be summed over all final neutron energies which can be reached with the reciprocal lattice point $\vec{\tau}$, and also summed over all reciprocal lattice points which contribute, consistent with momentum and energy conservation. The sum over final neutron energies is done by doing an integral over phonon wave vectors in references 1 and 5.

$$\sigma_{01}(E_1)^{\tau} = \frac{\pi^2 \hbar^2 S}{2MN B k_1^2} \iiint \frac{e^{-2W}}{\hbar\omega(e^{\hbar\omega/kT_1}-1)} |2\pi\vec{\tau}-\vec{f}| \frac{B}{(2\pi)^3} d^3f \quad (20)$$

The angular part of this integration is facilitated by the substitution⁵:

$$2\pi\tau - f = 2\pi\tau + \lambda f \quad -1 \leq \lambda \leq 1 \quad (21)$$

Substitution of 21 into 20 leads to

$$\sigma_{01}(E_1)^{\tau} = \frac{S \hbar^2 e^{-2W}}{16\pi\tau M k_1^2} \int_0^{f_M} \int_{\lambda_1}^{\lambda_2} \frac{(2\pi\tau + \lambda f)^2 e^{-2W}}{\hbar\omega(e^{\hbar\omega/k_0 T_1} - 1)} f^2 df d\lambda \quad (22)$$

The evaluation of the limits of integration, $\lambda_1, \lambda_2, f_M$, is carried out in references 1,5 on the basis of the Debye approximation. Equation 22, with the Debye approximation then gives the total one phonon up-scatter cross section contributed by the reciprocal lattice points $\vec{\tau}$. The equivalent phonon emission (down scattering) cross section is obtained by changing $(e^{h\omega/kT} - 1)$ to $(1 - e^{-h\omega/kT})$, ref. 1.

Equation 22 must be summed over all $\vec{\tau}$ which can contribute in order to obtain the total one phonon absorption cross section at energy E_1 ;

$$\sigma_{o_1}(E_1) = \sum_{\vec{\tau} \text{ allowed}} \sigma(E_1)^{\vec{\tau}} \quad (23)$$

The incoherent approximation is obtained by replacing the above sum over reciprocal lattice vectors $\vec{\tau}$ by an integration. This approximation should be better for neutrons of higher energy ($E_1 \sim k\theta_D$)¹, when many reciprocal lattice vectors contribute. The Debye temperature of the scattering material is θ_D .

$$\sum_{\vec{\tau}} \rightarrow 4\pi B \int \tau^2 d\tau \quad (24)$$

Using 24 in 19 and then integrating over f yields, according to ref. 1, the same result as would be obtained from treating the incoherent term in equation 16, except that R is replaced by S . The results for the total one phonon absorption cross section on the Debye approximation and the incoherent approximation is, according to Kothari and Singwi¹,

$$\sigma_{oi}(E_1)_{inc.} = \int_{\max(0, E_1 - k_0 \theta_D)}^{E_1 + k_0 \theta_D} \sigma_{i,m}(E_1 \rightarrow E_2) dE_2 \quad (25)$$

$$\sigma_{i,inc}(E_1 \rightarrow E_2) = \frac{3S \hbar^5 \omega}{16 m_0 M E_1 (k_0 \theta_D)^5 (e^{\hbar\omega/kT} - 1)} \int \frac{2m_0(\sqrt{E_2} + \sqrt{E_1})^2}{\hbar^2} y e^{-\alpha y/M} dy \frac{2m_0(\sqrt{E_2} - \sqrt{E_1})^2}{\hbar^2} \quad (26)$$

2. Multiphonon Processes

Multiphonon processes become important when the incident neutron energy approaches the Debye temperature ($E_1 \sim k\theta_D$) of the scattering material. At sufficiently high incident neutron energy the multiphonon cross section approaches the free atom cross section (ref. 1).

Treatments of the multiphonon cross section are usually done in the incoherent approximation because, so the arguments go, the relatively high neutron energy required to make multiphonon processes appreciable validates use of the incoherent approximation.

Cross sections for multiphonon processes can be obtained by modification of eq. 15¹. As many terms

$$\langle n_j - 1 | e^{i Q_j \sigma^{a_j} + Q_j^* \sigma^{a_j^*}} | n_j \rangle \quad (27)$$

are removed from the product in equation 15 as there are phonons absorbed by the neutron.

However, evaluation of the resultant equations are difficult, except on this basis of many approximations. Approximate expressions for multiphonon cross sections are given in numerous references, some of which are 1, 2, 6, 7, 8, 9, and 19.

3. Scattering Law

The scattering law is a way of combining the up-scatter and the down scatter cross sections into one formula in which the condition of detailed balance is explicitly taken into account, and was first introduced by Van Hove¹⁰.

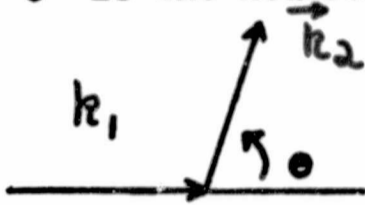
The double differential scattering cross section for neutrons scattering from an atomic system for a neutron wave vector change \vec{K} , and energy change $\pm \hbar\omega$ is written in terms of the scattering law as a product of a neutron term and an atomic term;

$$\frac{d^2 \sigma (E_1 \rightarrow E_2, \theta)}{dE_2 d\Omega} = \int \sqrt{\frac{E_2}{E_1}} \frac{e^{-\frac{E}{2}}}{4\pi} S(|\vec{K}| \hbar\omega) \quad (28)$$

$$\vec{K} = \vec{k}_1 - \vec{k}_2$$

Here $E_j = \frac{\hbar^2 k_j^2}{2m_0} \quad j = 1, 2$

θ is the neutron scattering angle



$$E_2 = E_1 + \epsilon$$

$$\epsilon = \pm \hbar \omega$$

Plus is for phonon absorption (neutron up-scatter).

Minus is for phonon emission (neutron down-scatter).

$S(|\vec{K}|, \hbar\omega)$ is the scattering law. In the polycrystalline case $S(\vec{K}, \hbar\omega)$ depends only upon E_1 , E_2 , and θ , that is, it is independent of the polar angle of \vec{k}_2 .

As an example of $S(\vec{K}, \hbar\omega)$ we re-write the one phonon absorption coherent differential cross section, equation 16 as

$$G_{01} = S \sqrt{\frac{E_2}{E_1}} \frac{e^{-\frac{\epsilon}{2}}}{4\pi} S_1(\vec{K}, \hbar\omega)$$

$$S_1(\vec{K}, \hbar\omega) = \frac{\hbar^2}{8\pi MN} \sum_{\vec{f}} e^{-2W} \sum_S (\vec{K} \cdot \vec{E}_S)^2 \frac{1}{\left[e^{\frac{\hbar\omega}{2kT}} - e^{-\frac{\hbar\omega}{2kT}} \right] \hbar\omega} \quad (29)$$

$$\frac{(2\pi)^3}{B} \delta(\vec{K} - 2\pi\vec{\tau} + \vec{f})$$

The subscript τ on $S_1(\vec{k}, \hbar\omega)$ indicates that the summation over reciprocal lattice vectors has not yet been performed.

The scattering law, equation 28, holds for all orders of phonon processes, with energy conservation generalized to:

$$E_2 = E_1 + \epsilon \quad (30)$$

and

$$\epsilon = \sum_{k=1}^n \sum_{l=1}^{n'} \hbar(\omega_k - \omega_l) \quad (31)$$

Where n is the number of phonons absorbed by the neutron and n' is the number of phonons emitted by the neutron during the scattering.

The scattering law is useful in experimental work in that data from up-scatter and down-scatter can be combined and averaged to give an experimental $S(|\vec{k}|, \hbar\omega)$. In calculations of scattering kernels, the scattering law makes it unnecessary to calculate both up-scatter and down-scatter, since the one can be easily obtained from the other through equation 29. Properties of $S(|\vec{k}|, \hbar\omega)$ are discussed in references 10, 11, and 12.

4. Considerations for Coherent Calculation

In order to calculate the double differential one phonon scattering cross section

$$\frac{d^2(E_1 \rightarrow E_2, \theta)}{dE_2 d\Omega} \quad (32)$$

it is necessary to sum $S_1(|\vec{k}|, \hbar\omega)$ (equation 29) over all phonon wave vectors

\vec{f} and all reciprocal lattice vectors $\vec{\tau}$, for a given $\hbar\omega$, consistent with the relation;

$$\vec{K} = 2\pi\vec{\tau} - \vec{f}$$

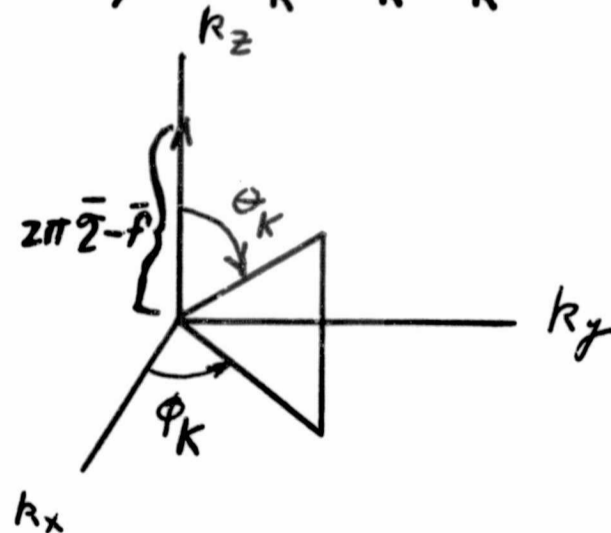
or $|k_1 - k_2| \leq |2\pi\vec{\tau} - \vec{f}| \leq k_1 + k_2$. (33)

With

$$\omega(\vec{f}) = \frac{1}{\hbar} (E_2 - E_1) = \omega(\vec{f} + 2\pi\vec{\tau})$$
 (34)

A polycrystalline average of equation 29 can be performed to obtain an expression useful in a coherent calculation of the one phonon cross section. The average is taken by neglecting the dependence of W on the orientation of \vec{K} relative to a microcrystal, and averaging the delta function of equation 29 over all angles between \vec{K} and the vector difference $2\pi\vec{\tau} - \vec{f}$. The y axis is taken along $2\pi\vec{\tau} - \vec{f}$.

$$I = \frac{1}{4\pi} \int_{\theta=0}^{\pi} \int_{\phi=0}^{2\pi} \delta(\vec{K} - 2\pi\vec{\tau} + \vec{f}) \sin\theta_K d\theta_K d\phi_K$$
 (35)



$$I = \frac{1}{4\pi} \int \int \delta(K_x) \delta(K_y) \delta(K_z - |2\pi\vec{\tau} - \vec{f}|) \frac{dk_x dk_y}{K^2 \cos \theta_K}$$

$$I = \frac{1}{4\pi} \frac{\delta(|\vec{K}| - |2\pi\vec{\tau} - \vec{f}|)}{|2\pi\vec{\tau} - \vec{f}|^2} \quad (36)$$

The polycrystal double differential one phonon scattering cross section becomes, from equation 29, 36:

$$\frac{d^2\sigma(E_1 \rightarrow E_2, \theta)}{dE_2 d\Omega} = S \sqrt{\frac{E_2}{E_1}} \frac{e^{-\frac{E}{2}}}{4\pi} S_1(K, \hbar\omega) \quad (37)$$

$$S_1(K, \hbar\omega) = \frac{\pi \hbar^2 e^{-2W}}{8MN} \sum_{\vec{f}} \sum_S \frac{|\vec{K} \cdot \vec{E}_S^{\vec{f}}|^2}{\left[\sinh \frac{\hbar\omega(\vec{f})}{2kT} \right] \hbar\omega(\vec{f})} \times \frac{\delta(|\vec{K}| - |2\pi\vec{\tau} - \vec{f}|)}{|2\pi\vec{\tau} - \vec{f}|^2} \quad (38)$$

Condition 34 defines surfaces of constant frequency within the first Brillouin zone centered about the reciprocal lattice point touched by $\vec{\tau}$. In order for a contribution to the scattering to arise from the first Brillouin zone surrounding the reciprocal lattice point $\vec{\tau}$, the sphere of radius $|\vec{K}|$ centered

about the reciprocal lattice origin must intersect the constant frequency surface $\omega(\vec{f})$. The intersection of the constant frequency surface with a sphere of radius $|\vec{K}|$ satisfied condition 33.

The summation over wave vectors along the intersection of the sphere and constant frequency surface must be done by an integration. The contributions at individual $\vec{\tau}$ vectors must be added to obtain the double differential cross section.

The value of W must be obtained from equation 6 by replacing the sum over wave vectors by an integration over the first Brillouin zone centered about the origin.

$$\sum_j \rightarrow \frac{B}{(2\pi)^3} \int_{\text{1st BZ.}} d^3\vec{f}. \quad (39)$$

However the variations of phonon polarization vectors $\vec{\epsilon}_s$ with phonon branch and location in the first Brillouin zone make evaluation of such an integral difficult. A simpler approximation for the evaluation of W is to assume that the polarization vectors are everywhere orthogonal, an assumption which is true for an isotropic homogenous solid but wrong for a hexagonal space lattice, and replace the sum by an integration over the frequency spectrum;

$$\sum_j \rightarrow \int_{\omega=0}^{\infty} g(\omega) d\omega \quad (40)$$

with the above assumption and 40, equation 6 becomes

$$2W = \frac{\hbar^2}{2MN} \vec{K}^2 \int_{\omega=0}^{\infty} \coth \frac{\hbar\omega}{2k_B T} \frac{g(\omega)}{\omega} d\omega \quad (41)$$

$g(\omega)$ is the lattice frequency distribution function. $g(\omega)$ gives the fraction of eigenfrequencies of the lattice which have frequency between ω and $\omega+d\omega$.

For normalization

$$\int_0^{\infty} g(\omega) d\omega = 1 \quad (42)$$

If a $g(\omega)$ function for the lattice is constructed, then the integration in 37 can be readily performed, although numerical techniques will, in general, have to be used.

The formulas so far have all been for lattices with one atom per unit cell. Generalizations to lattices with more than one atom per unit cell are straightforward. A form factor must be included in $S(\vec{k}, \hbar\omega)$ to account for the phase difference in scattering from various atoms in the unit cell, and sums over wave vectors must be over all $3n$ branches of the phonon spectrum¹, where n is the number of atoms in the unit cell.

Multiphonon processes would be difficult to calculate by explicit numerical integration over volumes of the first Brillouin zone. Authors seem to agree^{1,2,6,7,8,9,19}) that such an explicit calculation of multiphonon processes is not necessary. When the neutron energy is great enough to make multiphonon processes appreciable, it is great enough to make the incoherent approximation valid, is the argument. So the conclusion about multiphonon

processes is that they can probably be treated adequately by an incoherent approximation, and an approximation to the dispersion curves.

An incentive to perform a one phonon coherent calculation of the polycrystalline double differential scattering cross section for beryllium is the data of Schmunk¹³. He presents scattering law measurements for incident neutron energies from 0.04 to 0.10 ev.

Young and Koppel¹⁴ performed a coherent calculation for beryllium over a limited range of energy transfer and obtained reasonable agreement with Schmunk's¹³ data.

IV. LATTICE DYNAMICS AND SCATTERING LAW

1. General

The Harmonic approximation description of lattice dynamics is discussed in detail in many places^{3,15,16,17,18}. The approximation consists of replacing the forces between pairs of atoms of the crystal by two idealized components; a bond stretching force proportional to the first power of the change in distance from the equilibrium positions of the two atoms, and a bond bending force proportional to the change in angle between the equilibrium line joining the atoms and an arbitrary axis, that is proportional to the component of displacement perpendicular to the equilibrium line joining two atoms¹⁶. The total force acting on a particular atom is the sum of these two components arising from all of the other atoms of the crystal. The influence of other atoms of the crystal is usually taken in practice out to the third to the tenth shell of neighbors, although it could be taken to as many shells of neighbors as desired. The bulk compressibility of the electron gas of the solid can also be taken into account²⁰.

Force constants are introduced into the model. They usually are adjustable parameters. It would be possible to have three separate bond stretching force constants and three separate bond bending force constants for each atom whose influence is considered, in addition to three electron gas compressibilities. If three shells of neighbors from a hexagonally close packed (hcp) lattice were considered, and there are six neighbors per shell, then there could be a total of $3 \cdot 6 \cdot 6 = 108$ force constants plus the electron

gas compressibility. The features which distinguish different models of a lattice is how many shells of neighbors are considered and how many force constants are introduced.

Classical elasticity theory^{21,22} is used to derive¹⁶ relations between the atomic force constants. These relations can be used to evaluate atomic force constants from elasticity data, or as checks on the consistency of values obtained for the atomic force constants in other ways, for example, fitting by least squares to measured dispersion relations.

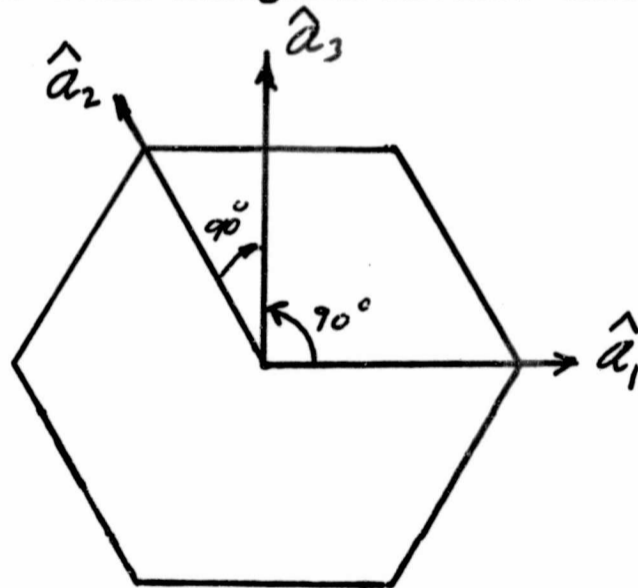
2. Beryllium

Several models proposed for beryllium will be compared. The crystal structure of beryllium is hexagonally close packed (hcp). The unit cell is a right hexagonal prism containing two identical atoms. If the origin of a unit cell is chosen at the position of one of the atoms, the two basis vectors are²³

$$\vec{r}_B(1) = 0$$

$$\vec{r}_B(2) = \frac{1}{3}\hat{a}_1 + \frac{2}{3}\hat{a}_2 + \frac{1}{2}\hat{a}_3$$

Here \hat{a}_1 , \hat{a}_2 , and \hat{a}_3 are the usual hexagonal lattice unit vectors, as shown in the sketch below.



A model of a hcp lattice developed by Begbie and Born²⁴, and by Begbie²⁵, includes interactions with nearest neighbors only. Seven atomic force constants are used in this model for both bond stretching and bond bending forces.

The hcp model of Slutsky and Garland²³ considers three shells of neighbors. The atomic interactions are taken to be bond stretching only, and three force constants are introduced, one for each shell of neighbors. The electron gas compressibility is also included as a parameter.

Collins²⁶ has developed a model for a hcp lattice and applied it to magnesium. The model goes to fourth nearest neighbors and introduces four independent force constants for each of the first three neighbor shells and two force constants for the fourth shell. Of the four constants one is for bond bending and three for bond stretching. In this general tensor model there are altogether fourteen independent force constants. Collins evaluated only nine of these constants using a combination of elasticity data and single phonon inelastic neutron scattering from a phonon of known polarization.

DeWames, Wolfram, and Lehman²⁷ have given a model of the hcp lattice. It is referred to as the modified axially symmetric model. They have applied it to beryllium and zinc. These authors include interactions out to the sixth shell of neighboring atoms and use three force constants for each shell of neighbors, one for bond stretching and two for bond bending. One of the bond bending force constants is for bending within the base plane and the other for bending out of the base plane, however, the ratio for these two bending constants is taken to be the same for each neighbor shell. So they actually

use two force constants for each shell plus the ratio of the two bending force constants, a total of thirteen constants for six shells of nearest neighbors. The relations of elasticity and crystal stability give relations between various groups of the atomic force constants, and these relations are met consistently by their numerical values.

Schmunk²⁸, et.al., measured the dispersion relation along several symmetry directions for beryllium by one phonon inelastic neutron scattering. They attempted to fit their data to the Begbie-Born model and the Slutsky-Garland model, both of which gave qualitative agreement. In order to achieve better quantitative agreement between their experiment and a model they extended the central force model of Slutsky and Garland to include interactions of the fourth and fifth neighbor shells. With this extended central force model they achieved a reasonable fit to their experimental data.

DeWames²⁷, et.al., obtained a better fit to the data of Schmunk²⁸, et.al. with their model than the extended Slutsky-Garland model gave.

Young²⁹ and Young and Koppel³⁰ used the extended Slutsky-Garland model with the force constants obtained by Schmunk²⁸, et.al. to calculate the frequency distribution of beryllium. From their frequency distribution they calculated the polycrystalline inelastic neutron scattering cross section both in the incoherent approximation^{31,29} and in a coherent calculation of one phonon processes³² for small energy transfer. This latter calculation compares favorably with the polycrystalline inelastic double differential neutron scattering measurements made by Schmunk³³.

A comparison of beryllium double differential inelastic scattering cross section measurements made by Sinclair with calculations based on the incoherent approximation is given by Young and Koppel³¹. The calculations were made by the code SUMMIT³⁶ using the frequency spectrum obtained from the extended Slutsky-Garland model by Young and Koppel³¹. The calculation misses the data points at low momentum transfer where interference effects are important. No comparison has been made between an incoherent calculation and the data of Schmunk³³. Young and Koppel³² have made a comparison of their low energy transfer coherent calculation and Schmunk's³³ data. If this calculation³² were developed into a full scattering kernel, it would allow an accurate evaluation of the role of coherent inelastic scattering on the operation of cold beryllium moderated reactors.

A more accurate numerical method for the incoherent approximation than was used in the code SUMMIT³⁶ has been written into a pair of codes called GASKET and FLANGE⁴² by people at General Atomics. Beryllium kernels calculated on the basis of these two codes should be available in the future from the Brookhaven National Laboratory Evaluated Nuclear Data File (ENDF)⁴³. A copy of the FLANGE code was given to the author by Dr. J. A. Young and Dr. John Neil, both of General Atomics.

3. Graphite

The crystal structure³⁷ of graphite is hexagonal with four atoms per unit cell. It tends to form into weakly coupled plane sheets with atoms arranged in hexagons.

A Born-von Karman model of graphite has been developed by Yoshimori and Kitano³⁷. Their model includes the anisotropy of the graphite lattice, by including four force constants; the first for bond stretching in the base planes, the second for bond bending in the base planes, the third for bond stretching along the C axis, and the fourth for the displacement of an atom out of a base plane. Only first neighbor interactions are considered.

Calculation of a scattering kernel for graphite using the frequency spectrum of Yoshimori and Kitano³⁷ is presented by Wilkner³⁸, et.al. They used the incoherent approximation, the code SUMMIT³⁶, for their calculation. Wilkner³⁸, et.al. give a comparison of their calculation with the measurement of the inelastic graphite scattering law by Egelstaff³⁹. The agreement is good, except for interference effects at low momentum transfer where the incoherent approximation is expected to fail. Wilkner³⁸, et.al. state that reactor parameters calculated on the basis of their kernel agree also with experiment.

Young and Koppel⁴⁰ have derived a more accurate graphite frequency spectrum using the model of Yoshimori and Kitano³⁷ than was obtained by Yoshimori and Kitano³⁷. Young and Koppel used the root sampling technique which is a better numerical method than was employed by Yoshimori and Kitano. Young⁴¹, et.al. have compared scattering kernels computed using their new

frequency spectrum and the one computed by Wilkner, et.al., and reached the conclusion that the two scattering kernels are nearly identical. However, measurements by Whittemore⁴⁴ apparently show a discrepancy in the predictions of the Young-Koppel calculation.

A copy of the GASKET⁴² computed scattering law for 296°K graphite was given to the author by Dr. J. A. Young and Dr. John Neil, both of General Atomic. With the copy of FLANGES⁴² also given to the author by the above two people, a kernel up to 1.0 ev was computed on the WANL TNS fine mesh. However this kernel has not been put on the TNS library tapes, to date.

4. Method of Calculating the Frequency Distribution $g(\omega)$

The Born model of lattice vibrations discussed in Section 1 above leads to a set of coupled linear homogenous algebraic equations, the solution to which can be written in the determinant form;

$$\left| D(\vec{k}) - \omega^2 \mathbf{I} \right| = 0 \quad (42)$$

If there are n atoms per unit cell of the crystal lattice, $D(\vec{k})$ and \mathbf{I} are $3n \times 3n$ matrices. $D(\vec{k})$ is the dynamical matrix of the lattice and \mathbf{I} is the unit matrix. The eigenvalues of $D(\vec{k})$ are ω_j^2 where j indicates one of the $3n$ roots, and the ω_j are the eigenfrequencies of the lattice. The elements of the matrix $D(\vec{k})$ depend upon the geometry of the lattice, the model and atomic force constants, and the wave vector \vec{k} of the vibration. In the papers quoted in Section 2 above explicit formulas for the elements of $D(\vec{k})$ are worked out on the basis of the different models.

The frequency distribution function is a very useful function and is necessary for the approximate evaluation of sums over all eigenmodes of the lattice. A chapter in Reference 3 explains several methods for calculating the frequency distribution function $g(\omega)$. The calculational method often adopted is to divide the first Brillouin zone into many small prisms of the symmetry of the unit cell, to evaluate the matrix $D(\vec{k})$ at the center of each prism, find the eigenvalues ω_j^2 at the center of each prism, and to compile a histogram of the number of eigenvalues between ω and $\omega + \Delta\omega$. The histogram is then the frequency distribution function $g(\omega)$. This procedure is known as the root sampling method. The frequency distribution function is usually normalized so that;

$$\int_0^{\infty} g(\omega) d\omega = 1. \quad (43)$$

An improvement on the root sampling method has been reported by Gilat and Raubenheimer³⁴. These authors calculate the eigenvalues of $D(\vec{k})$ at the center of many small prisms within the first Brillouin zone, just as in the root sampling method. However, they also expand the eigenvalue about the center of the prism in a Taylor expansion, keeping only the linear term, and extrapolate throughout the small prism in order to determine the fraction of the volume of the small prism contained between surfaces of constant eigenvalue. The surfaces of constant eigenvalue are approximated within a small prism by planes. The contribution of each small prism to the histogram channel between ω and $\omega + \Delta\omega$ is then determined, and the contributions from each cube added. With this technique of extrapolation they are able to get much better

resolution on the histogram than is available in a standard root sampling technique. They have worked out the calculation in detail only for cubic lattices, simple cubic, body centered cubic, and face centered cubic. For a given resolution on the $g(\omega)$ histogram the Gilat-Raubenheimer extrapolation method should require fewer mesh points in the first Brillouin zone than does the straight root sampling technique, with a consequent saving in computer time.

V. CONCLUSIONS

The review of the literature concerning calculations and measurements of inelastic double differential neutron scattering cross section for polycrystalline beryllium and graphite shows that rather accurate scattering kernels calculated on the basis of the incoherent approximation have been obtained for room temperature. Calculations on the incoherent approximation are available for many temperatures. J. A. Young, et.al. are continuing work on coherent calculations for both materials. Calculation of coherent inelastic scattering should be pursued in order to determine the effect of coherent scattering in cold (100°K) beryllium on the operation of a NERVA type reactor. Since a NERVA type reactor uses cold beryllium, it would be good to have available low temperature (liquid nitrogen temperature $\sim 77^\circ\text{K}$) measurements of inelastic polycrystalline scattering law.

REFERENCES

1. Kothari, L. S. and Singwi, K. S., Solid State Physics, Vol. 8, Editors Seitz and Turnbull, Academic Press, New York, 1959.
2. Kothari, L. S. and Duggal, V. P., Advances in Nuclear Science and Technology, Vol. 2, p. 194, Academic Press, New York, 1964.
3. Maradudin, A. A., Montroll, E. W., Weiss, G. H., The Theory of Lattice Dynamics in the Harmonic Approximation, Solid State Physics, Supplement 3, Editors Seitz and Turnbull, Academic Press, New York, 1963.
4. Hughes, D. J., Pile Neutron Research, Addison-Wesley, Cambridge, 1953.
5. Weinstock, R., Phys. Rev. 65, 1 (1944).
6. Söjlander, A., Arkiv. För Fysik, Band 14 nr. 21, 315 (1958).
7. Placzek, G., Phys. Rev. 93, 895 (1954).
8. Placzek, G., Phys. Rev. 105, 1240 (1957).
9. Lomer, W. M. and Low, G. G., Thermal Neutron Scattering, Editor P. A. Egelstaff, p. 1, Academic Press, 1965.
10. Van Hove, L., Phys. Rev. 95, 249 (1954).
11. Nelkin, M., Inelastic Scattering of Neutrons in Solids and Liquids, IAEA Conference, Vienna, 1960, p. 3, IAEA Vienna 1961.
12. Egelstaff, P. A., See reference 11, page 25.
13. Schmunk, R. E., Phys. Rev. 136, A1303 (1964).
14. Young, J. A., Koppel, J. U., General Atomics Report, GA-6238, 1965, (to be published).
15. Born, M. and Huang, K., Dynamical Theory of Crystal Lattices, Oxford, London, 1956.
16. deLaunay, J., "The Theory of Specific Heats and Lattice Vibrations", Vol. 2, Solid State Physics, Editors Seitz and Turnbull, Academic Press, New York, 1959.
17. Ziman, J. M., Electrons and Phonons, Oxford, 1960.
18. Ziman, J. M., Principles of the Theory of Solids, Oxford, London, 1964.

19. Marshall, W. and Stuart, R. N., University of California Lawrence Radiation Laboratory Report UCRL-5568, (1959).
20. deLaunay, J., Reference 16, pages 276-285.
21. Joos, J., Theoretical Physics, third edition, Hafner, New York, 1958.
22. Sommerfeld, A., Mechanics of Deformable Bodies, Lectures on Theoretical Physics, Vol. 2, Academic Press, New York, 1964.
23. Slutsky, L. J. and Garland, C. W., J. Chem. Phys. 26, 787 (1957).
24. Begbie, G. H. and Born, M., Proc. Royal Society (London) A188, 179 (1946).
25. Begbie, G. H., Proc. Royal Soc. (London) A188, 189 (1946).
26. Collins, M. F., Proc. Phys. Soc. (London) 80, 362 (1962).
27. DeWames, R. W., Wolfram, G., and Lehman, G. W., Phys. Rev. 138, A717 (1965).
28. Schmunk, R. W., Brugger, R. M., Randolph, P. D., and Strong, K. A., Phys. Rev. 128, 562 (1962).
29. Young, J. A., General Atomics Report No. GA-4638 (1963).
30. Young, J. A. and Koppel, J. U., Phys. Rev. 134, A1476 (1964).
31. Young, J. A. and Koppel, J. U., Nucl. Sci. and Eng. 19, 367-373 (1964).
32. Young, J. A. and Koppel, J. U., reference 14.
33. Schmunk, R. E., Reference 13.
34. Gilat, G. and Raubenheimer, L. J., Phys. Rev. 144, 390 (1966).
35. Sinclair, R. N. Proc. of the Symposium on Inelastic Scattering of Neutrons in Solids and Liquids, Chalk River, Canada, 1962, Vol. 2, p.199, IAEA, Vienna, 1963.
36. Bell, J., General Atomics, GA-2492 (1962).
37. Yoshimori, A. and Kitano, J., Phys. Soc. Japan 2, 352 (1956).
38. Wilkner, N. F., Joanou, G. D., Parks, D. E., Nucl. Sci. and Eng. 19, 108 (1964).

39. Egelstaff, P. A., Compilation of Early Scattering Law Data, Atomic Energy Research Establishment Report, AERE-R-3931 (1962).
40. Young, J. A. and Koppel, J. U., J. Chem. Phys. 42, 357 (1965).
41. Young, J. A., Wilkner, N. F., Parks, D. E., Genral Atomics Report, GA-6075 (1965).
42. Beyster, J. R., Brown, J. R., Corngold, N., etc., General Atomics, Integral Neutron Thermalization Annual Summary Report, October 1963 through September 1964, GA-5798.
43. ENDF Evaluated Nuclear Data File, Brookhaven National Laboratory Report No. BNL-8381 (1964) and newsletters.
44. Whittmore, W. L. Symposium on Inelastic Scattering of Neutrons by Condensed Systems, p. 94, BNL-940(C-45), 1965.